Electronic Supplementary Information (ESI) for

Reduced Graphene Oxide/Mixed-valent Manganese Oxides Composite Electrode for Supercapacitors with High Capacitance and Super-Long Life

Yang Wang,[a] Wenhui Lai,[a] Ni Wang,[b] Zhi Jiang,[a] Xuanyu Wang,[a] Peichao Zou,[a] Ziyin Lin,[c] Hongjin Fan,[d] Feiyu Kang,[a] and Ching-Ping Wong,[c] Cheng Yang[a*]

[a] *Division of Energy and Environment, Graduate School at Shenzhen, Tsinghua University, Shenzhen 518055, China; E-mail: yang.cheng@sz.tsinghua.edu.cn*

[b] *State Key Laboratory of Electronic Thin Films and Integrated Devices, University of Electronic Science and Technology of China, Chengdu 610054, China;*

[c] *School of Materials Science and Engineering, Georgia Institute of Technology, 771 Ferst Drive, Atlanta, Georgia 30332, United States*

[d] *School of Physical & Mathematical Sciences, Nanyang Technological University, Singapore*

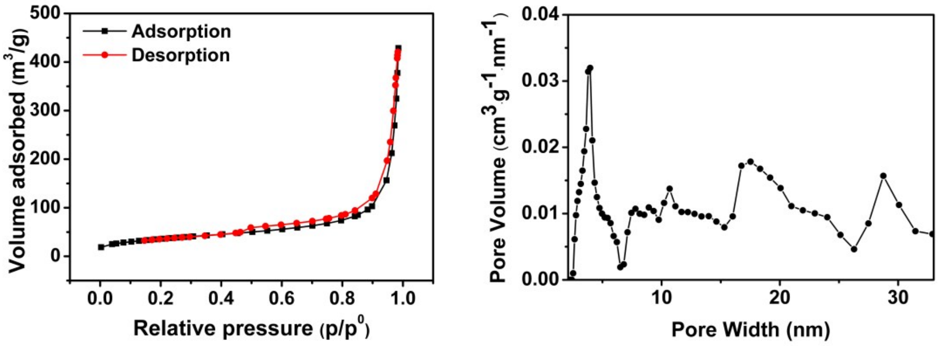

Fig.S1 Adsorption isotherm of rGO/MnO_x composite.

Adsorption isotherm of the rGO/MnO_x composite is shown as Fig. S1, from which we can see that the pore size distribution of this composite is 2-36 nm with an average pore size of 20.2 nm.

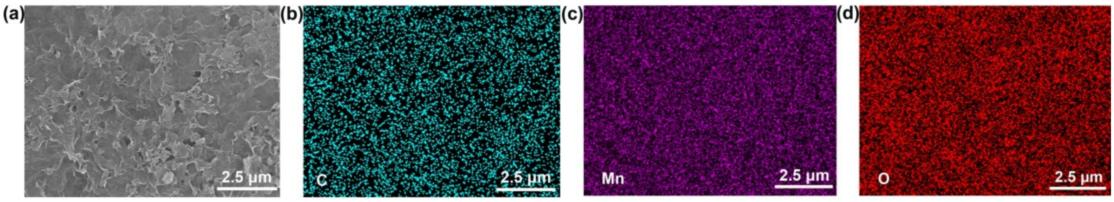

Fig.S2 SEM image (a) of GO/MnO_2 combined with EDS mapping in the same area and relative intensities of C (b), Mn (c), and O (d) elements.

Fig. S2 a-d is the SEM image combined with EDS mapping of the GO/MnO_2 composite in the same area and relative intensities of C (b), Mn (c), and O (d) elements. As can be seen, the three elements bestrewed over the whole area, further confirming that the two components were evenly distributed in the composite.

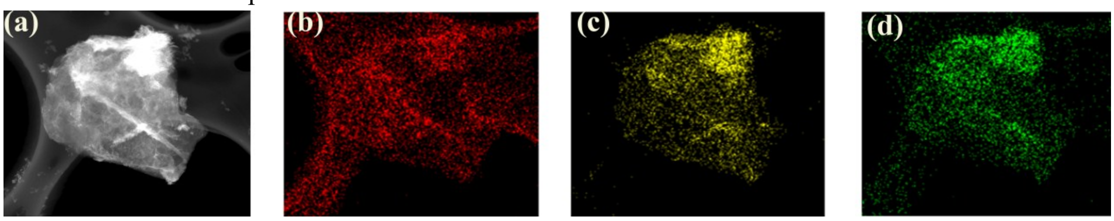

Fig. S3 HAADF TEM image (a) of GO/MnO_2 combined with EDS mapping in the same area and relative intensities of C (b), O(c), and Mn (d) elements.

Fig. S3 a-d is the HAADF TEM image combined with EDS mapping of the GO/MnO_2 composite in the same area and relative intensities of C (b), Mn (c), and O (d) elements. As we can see, the three elements distributed evenly over the whole area.

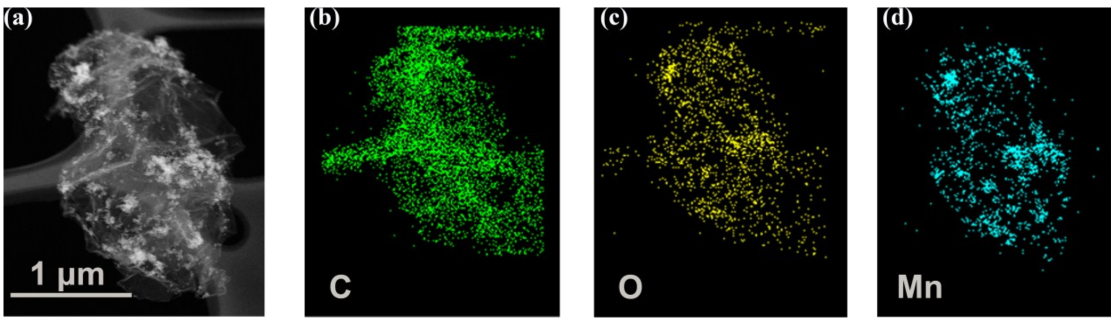

Fig. S4 HAADF TEM image (a) of rGO/MnO_x combined with EDS mapping in the same area and relative intensities of C (b), O(c), and Mn (d) elements.

Fig. S4 a-d is the HAADF TEM image combined with EDS mapping of the rGO/MnO_x composite in the same area and relative intensities of C (b), O (c), and Mn (d) elements. As we can see, the three elements distributed evenly over the whole area.

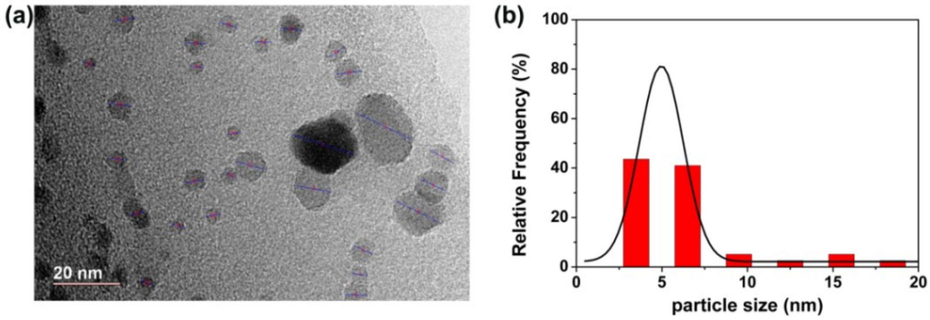

Fig. S5 (a) High-magnification TEM image of the rGO/MnO_x composite; (b) Size distribution of MnO_x particle.

Fig. S5 are the high-magnification TEM image of the rGO/MnO_x composite and the MnO_x particle distribution on the rGO sheet. As we can see, the MnO_x particle distribute evenly onto the rGO sheet with the particle size ranging from 3 to 20 nm.

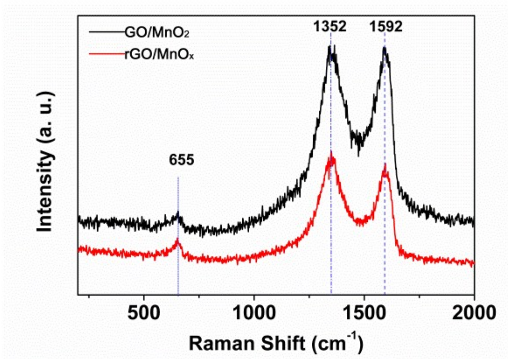

Fig. S6 The change in the Raman spectra before and after the reduction.

Fig. S6 shows the change in the Raman spectra of the composite before and after the reduction, the weak Raman shift at the peaks of 655 cm^{-1} represented the stretching vibration of the M-O bond in the manganese oxides, the bands at 1352 and 1592 cm^{-1} evidently came from the GO and rGO sheets.

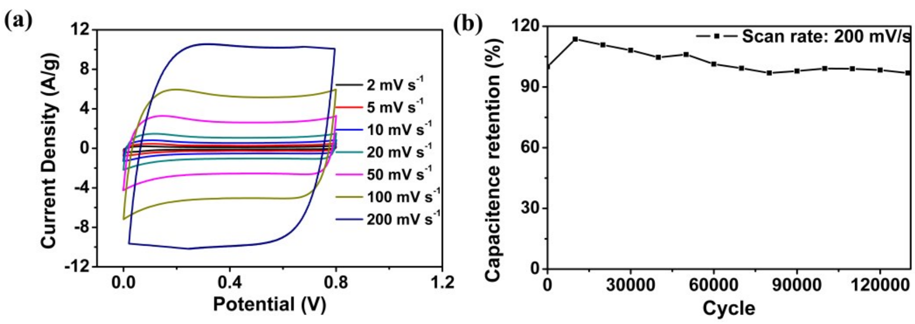

Fig. S7 Electrochemical performance of the AC electrode material.

Fig. S7 shows the electrochemical performance of the AC electrode. Based on 0.5 M Na_2SO_4 electrolyte, the C_m value of AC electrode was 80 F g^{-1} at the scan rate of 2 mV s^{-1}, and exhibited a good rate performance at the scan rates ranging from 2 to 200 mV s^{-1}. The capacitance retention was 97% after 130000 charge-discharges, revealing good cycling stability of the AC electrode.

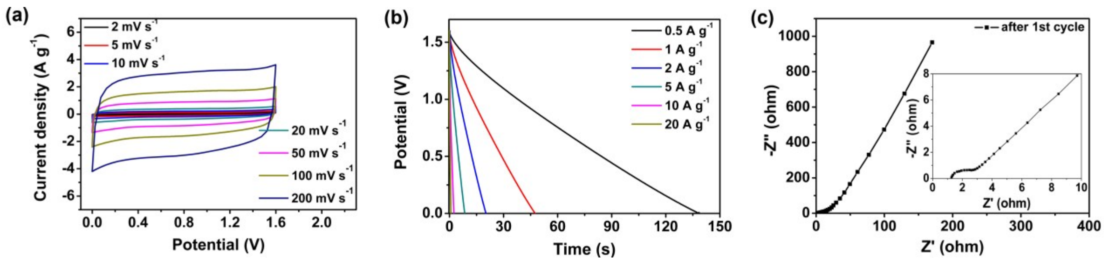

Fig. S8 CV (a), GD (b) and EIS (c) performances of the asymmetric supercapacitor based on 0.5 M Na_2SO_4 electrolyte.

Electrochemical performance of the ASc based on 0.5 M Na_2SO_4 electrolyte was investigated with the voltage window of 0 to 1.6 V, results are displayed as Fig. S8. Therein, the CV plot of the ASc is shown in Fig. 8Sa, with the scan rate ranging from 2 to 200 mV s^{-1}. As we can see, the curves exhibited as nearly rectangular shapes with weak redox peaks. This phenomenon was corresponded to the GD curves of the device, which were investigated with the current density of 0.5-20 A g^{-1}, shown in Fig. 8Sb. EIS was employed to study the impedance performance of the device, shown in Fig. 8Sc, conducted in the frequency range between 0.01 Hz and 100 kHz with amplitude of 5 mV at an open-circuit potential. Inset is the magnified data of the high frequency range, from which the equivalent series resistance can be calculated as 1.3 Ω, which suggested that the electrode exhibit a good conductivity.

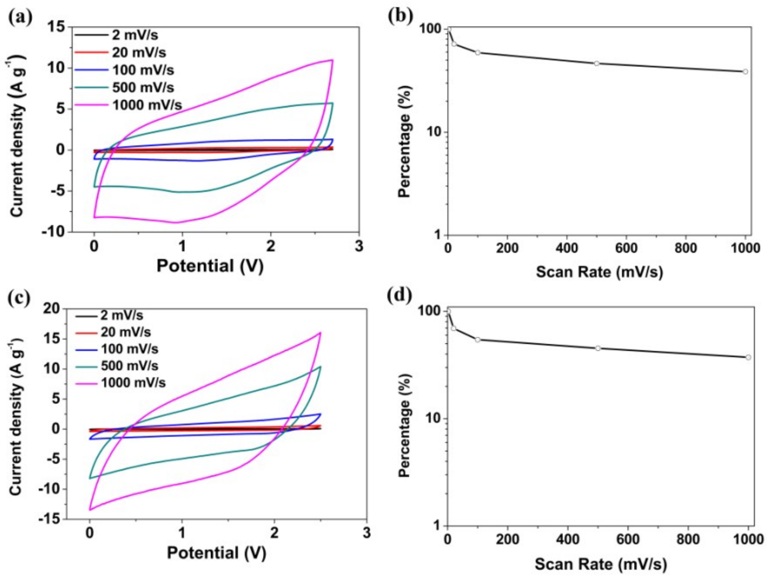

Fig. S9 Electrochemical data of the tailorable and surface mountable ASCs. (a) and (c) are the CV data of tailorable and surface mountable ASCs, respectively; (b) and (d) are the plots of capacitance retention values versus scanning rate calculated by CV study of the tailorable surface mountable ASCs, respectively

The electrochemical data of the tailorable and surface mountable devices are shown in Fig. S9. Ionic liquid $[C_2MIm]BF_4$ was used as the electrolyte, to elevate the working voltage window of the AScs up to 0-2.7 V. The rate-dependent CV characterizations of the AScs were performed under various scan rates ranging from 2-1000 mV s^{-1}, and the devices exhibited excellent rate performance at the tested scan rate range. The results are similar to that of Fig. 5 in the main text, which further prove the reliability of the devices' package schemes.

Table S1. Summary of some basic properties of various AScs.

Electrode materials	Electrolyte	Operation voltage (V)	E_{max} (Wh/kg)	P_{max} (kW/kg)	Stability (cycles)	Ref.
Bi_2O_3 //MnO_2 -ASc	Na_2SO_4	1.8	11.3	3.37	85% (1000th)	[1]
graphene//MGC	Na_2SO_4	2.0	30.4	5	79% (1000th)	[2]
CNT–CM//ACNF	Na_2SO_4	2.0	30.6	20.8	94% (5000th)	[3]
3DG/AC// 3DG/CNTs/MnO_2	Na_2SO_4	2.0	33.71	22.7	95.3% (1000th)	[4]
AGMn//aMEGO	Na_2SO_4	2.0	32.3	24.5	80.5% (5000th)	[5]
GNR// GNR–MnO_2 (18%)	Na_2SO_4	2.0	29.4	25.9	88% (5000th)	[6]
AC//Co_3O_4	KOH	1.6	36	8	89% (2000th)	[7]
Graphene/CF// MnO_2 /CF	PVA/ LiCl	1.5	27.2	6	95.2% (3000th)	[8]
GA//MGA	Na_2SO_4	1.6	17.8	3.2	84.1% (2000th)	[9]
HPC//MnO_2/GO	Na_2SO_4	2.0	46.7	2	93% (4000th)	[10]
$FeCo_2S_4$-$NiCo_2S_4$// $FeCo_2S_4$-$NiCo_2S_4$	KOH/PVA	1.0	46	4.72	92% (3000)	[11]
AC//$MnCo_2O_4$@ $Ni(OH)_2$	KOH	1.6	48	14.9	90% (2500)	[12]
$NiCo_2S_4$@PPy-50//AC	KOH	1.6	34.62	12	80.64% (2500)	[13]
AC//rGO/MnO_x	$[C_2MIm]BF_4$	2.7	47.9	20.8	96% (80000th)	This work

References

1. H. Xu, X. Hu, H. Yang, Y. Sun, C. Hu and Y. Huang, *Adv. Energ. Mater.*, 2015, **5**, 1401882.
2. Z. S. Wu, W. Ren, D. W. Wang, F. Li, B. Liu and H. M. Cheng, *ACS Nano*, 2010, **4**, 5835-5842.
3. J.-G. Wang, Y. Yang, Z.-H. Huang and F. Kang, *Carbon*, 2013, **61**, 190-199.
4. W. Chen, Y. He, X. Li, J. Zhou, Z. Zhang, C. Zhao, C. Gong, S. Li, X. Pan and E. Xie, *Nanoscale*, 2013, **5**, 11733-11741.
5. X. Zhao, L. L. Zhang, S. Murali, M. D. Stoller, Q. H. Zhang, Y. W. Zhu and R. S. Ruoff, *ACS Nano*, 2012, **6**, 5404-5412.
6. M. Liu, W. W. Tjiu, J. Pan, C. Zhang, W. Gao and T. Liu, *Nanoscale*, 2014, **6**, 4233-4242.
7. R. R. Salunkhe, J. Tang, Y. Kamachi, T. Nakato, J. H. Kim and Y. Yamauchi, *ACS Nano*, 2015, **9**, 6288-6296.
8. N. Yu, H. Yin, W. Zhang, Y. Liu, Z. Tang and M.-Q. Zhu, *Adv. Energ. Mater.*, 2016, **6**, 1501458.
9. Y. Liu, D. He, H. Wu, J. Duan and Y. Zhang, *Electrochim. Acta*, 2015, **164**, 154-162.
10. Y. Zhao, W. Ran, J. He, Y. Huang, Z. Liu, W. Liu, Y. Tang, L. Zhang, D. Gao and F. Gao, *Small*, 2015, **11**, 1310-1319.
11. J. Zhu, S. Tang, J. Wu, X. Shi, B. Zhu and X. Meng, *Adv. Energ. Mater.*, 2016, 1601234.
12. Y. Zhao, L. Hu, S. Zhao and L. Wu, *Adv. Funct. Mater.*, 2016, **28**, 1-9.
13. M. Yan, Y. Yao, J. Wen, L. Long, M. Kong, G. Zhang, X. Liao, G. Yin and Z. Huang, *ACS Appl Mater Interfaces*, 2016, **8**, 24525-24535.